BIOCHEMISTRY
including biophysical chemistry & molecular biology

Article

pubs.acs.org/biochemistry

Binding by the Hepatitis C Virus NS3 Helicase Partially Melts Duplex DNA

Veronica M. Raney,[†,§] Kimberly A. Reynolds,[†] Melody K. Harrison,[†,∥] David K. Harrison,[†] Craig E. Cameron,[‡] and Kevin D. Raney*[,†]

[†]Department of Biochemistry and Molecular Biology, University of Arkansas for Medical Sciences, Little Rock, Arkansas 72205, United States

[‡]The Pennsylvania State University, University Park, Pennsylvania 16802, United States

Supporting Information

ABSTRACT: Binding of NS3 helicase to DNA was investigated by footprinting with $KMnO_4$, which reacts preferentially with thymidine residues in single-stranded DNA (ssDNA) compared to those in double-stranded DNA (dsDNA). A distinct pattern of reactivity was observed on ssDNA, which repeated every 8 nucleotides (nt) and is consistent with the known binding site size of NS3. Binding to a DNA substrate containing a partial duplex was also investigated. The DNA contained a 15 nt overhang made entirely of thymidine residues adjacent to a 22 bp duplex that contained thymidine at every other position. Surprisingly, the $KMnO_4$ reactivity pattern extended from the ssDNA into the dsDNA region of the substrate. Lengthening the partial duplex to 30 bp revealed a similar pattern extending from the ssDNA into the dsDNA, indicating that NS3 binds within the duplex region. Increasing the length of the ssDNA portion of the partial duplex by 4 nt resulted in a shift in the footprinting pattern for the ssDNA by 4 nt, which is consistent with binding to the 3′-end of the ssDNA. However, the footprinting pattern in the dsDNA region was shifted by only 1−2 bp, indicating that binding to the ssDNA−dsDNA region was preferred. Footprinting performed as a function of time indicated that NS3 binds to the ssDNA rapidly, followed by slower binding to the duplex. Hence, multiple molecules of NS3 can bind along a ssDNA−dsDNA partial duplex by interacting with the ssDNA as well as the duplex DNA.

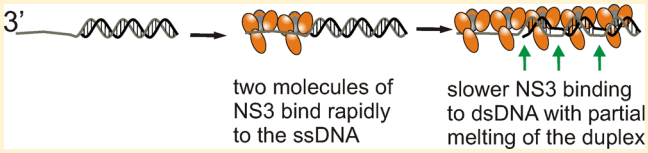

Helicases are molecular motor proteins that use ATP hydrolysis to manipulate nucleic acids.[1−4] Helicases disrupt nucleic acid structure as well as remodel protein−nucleic acid complexes. The role of helicases in virtually all nucleic acid metabolic events has led to in-depth investigations into the mechanism(s) of these enzymes.[5] One of the most studied helicases is NS3 from the hepatitis C virus (HCV).[6−8] The helicase activity of NS3 is required for replication of the HCV genome based on studies using a subgenomic replicon that encodes the HCV nonstructural proteins.[9] However, the specific role in HCV viral multiplication played by this enzyme has not been delineated. HCV infection causes chronic liver disease and hepatocellular carcinoma, so understanding the specific role and mechanism of NS3 has significant medical importance. The extensive study of NS3 has made this enzyme a model system for understanding the detailed biochemical mechanism for how helicases manipulate nucleic acids.

Helicases are categorized into several superfamilies based on sequence comparisons.[10,11] NS3 is in superfamily 2, which shares basic structural elements with superfamily 1 helicases, including the Walker A and Walker B regions that participate in binding and hydrolysis of ATP. NS3 is further classified as a DExH motor protein. The helicase motifs are located within two RecA-like domains forming a cleft in which ATP binding and hydrolysis occur.[12] The two domains are known to move closer together upon binding ATP and then separate after ATP hydrolysis.[13,14] The movement of these domains coordinates specific amino acid interactions with the nucleic acid that lead to directionally biased movement along the RNA or DNA strand.[15,16]

Many helicases exhibit a preference for nucleic acid substrate, operating on DNA or RNA, but not necessarily both. Although RNA is believed to be the biological substrate for NS3, this enzyme also functions equally well on DNA in vitro.[9,17] At present, there is no known biological role for NS3 functioning on DNA, although the protein has been found in the nuclei of patients infected with HCV.[18,19] Characterization of the DNA binding and unwinding activities of NS3 has significance for our overall understanding of how this model system selects specific nucleic acid structures. Previous studies suggest that NS3 interacts with the nucleic acid substrate at a single-stranded−double-stranded (ss−ds) junction,[20] but structural characterization of this interaction is lacking.

Biophysical and kinetic experiments indicate that NS3 can interact with itself in vitro and that oligomers[17] or dimers[21] are responsible for optimal unwinding of short DNA or RNA substrates, respectively. A monomeric form is also capable of unwinding DNA[22] and RNA.[23] Previous work suggested that

Received: May 22, 2012
Revised: August 17, 2012
Published: August 23, 2012

the DNA substrate was coated by NS3 molecules under conditions in which optimal DNA unwinding was observed.[17] Multiple molecules of NS3 or the helicase domain (NS3h) have been proposed to line up along the ssDNA portion of a partial duplex substrate and function together to enhance DNA unwinding activity.[24] This phenomenon has been termed functional cooperativity. In this report, the spatial orientation and number of NS3 molecules bound to ssDNA and partial duplex substrates have been investigated by DNA footprinting using $KMnO_4$. Results indicate that the binding energy of the enzyme predisposes the duplex DNA for melting. A model whereby multiple molecules of NS3 bind to the DNA substrate and participate in the binding and unwinding process is proposed.

MATERIALS AND METHODS

DNA oligonucleotides were from Integrated DNA Technologies (Coralville, IA) and purified by preparative gel electrophoresis. [γ-^{32}P]ATP was purchased from PerkinElmer Life Sciences. T4 polynucleotide kinase was obtained from New England Biolabs. HEPES, BME, SDS, MOPS, Tris, NaCl, Na_4EDTA, BSA, acrylamide, bisacrylamide, $MgCl_2$, KOH, ATP, formamide, xylene cyanol, bromophenol blue, urea, $KMnO_4$, glycerol, and $MgCl_2$ were purchased from Fisher. Streptavidin Dynabeads were from Invitrogen.

Recombinant full-length NS3 was derived from the HCV Con 1b replicon consensus sequence. NS3 was expressed as a fusion protein with a sumoylation tag (SUMO) on the N-terminus. Protein purification was performed by initially capturing expressed protein on a nickel affinity column via a His_6 tag on the N-terminus of the SUMO fusion. The SUMO fusion protein was cleaved by incubation with Ulp 1 protease, followed by a second round of nickel affinity chromatography. Final polishing of NS3 was performed by heparin Sepharose and anion exchange chromatography as described previously.[17]

DNA Footprinting with $KMnO_4$. DNA footprinting reactions were modified from a procedure established by Bui et al.[25] DNA oligonucleotide substrates were designed with a biotin label located adjacent to the 5′-end. A nucleotide was placed at the 5′-end for radiolabeling with ^{32}P. Footprinting reactions were performed at 37 °C in buffer consisting of 25 mM MOPS (pH 7.0), 50 mM NaCl, 10 mM $MgCl_2$, and 0.2 mg/mL BSA. Aqueous $KMnO_4$ (100 mM) was stored frozen at −80 °C and thawed immediately prior to use. Radiolabeled DNA substrates (10 nM) in buffer were incubated with NS3 (concentrations listed in figure legends) for 9 min at 37 °C followed by addition of $KMnO_4$ to a final concentration of 3.3 mM. The footprinting reaction proceeded for 5 s followed by quenching upon addition of 1 M BME and 200 mM EDTA. M-280 streptavidin Dynabeads (0.04 mg/mL) were added to the solution, and the mixture was vortexed at room temperature for 30 min. DNA-bound Dynabeads were captured by magnetic isolation, suspended in a solution (100 μL) containing 1 M piperidine and 0.1 mM biotin, and heated to 90 °C for 30 min. Dynabeads were removed, and the solution was evaporated using a SpeedVac. The dried residue was dissolved in 30 μL of H_2O and re-evaporated twice to remove residual piperidine. The DNA samples were suspended in denaturing buffer (95% formamide, 0.025% SDS, 0.025% xylene cyanol, and 0.025% bromophenol blue) and separated by electrophoresis on a denaturing 20% polyacrylamide gel. The DNA bands were quantifed by using a Typhoon PhosphorImager and ImageQuant (GE Healthcare, Piscataway, NJ). The footprinting data were analyzed by determining the radioactivity in each band corrected for background in triplicate experiments. The sum total radioactivity in each lane was determined, and the fraction of the total in each individual band was calculated. The fraction of radioactivity for each band in the presence of NS3 was divided by the fraction in the absence of NS3 to obtain "thymidine reactivity", which represents the relative reactivity of each thymidine position with permanganate in the presence and absence of NS3.

RESULTS

NS3 Binding to ssDNA Results in a Repeating Pattern of High Reactivity and Protection toward $KMnO_4$. The binding of NS3 to DNA has been determined for various forms of the enzyme. Most quantitative binding data have been obtained using only the helicase domain (NS3h). Binding of NS3h to ssDNA (12mer) has resulted in a K_D value of 10 nM, whereas binding to a duplex resulted in a K_D value of 1 μM.[20] Additional experiments support specific binding of NS3h to a ssDNAQ−dsDNA junction or a "fork" structure.[20] However, NS3h is not directly comparable to NS3, because the presence of the protease domain changes the affinity for nucleic acid. Full-length NS3 has been examined for binding using fluorescence anisotropy and electrophoretic mobility shift assays (EMSAs). The K_D value for binding to a 15mer ssDNA was 4.7 nM, whereas binding to a blunt end duplex of 30 bp resulted in a K_D value of 16 nM.[17] Hence, NS3 behaves quite differently than NS3h in binding to duplex DNA. It should be noted that different genotypes of NS3 behave differently in binding and activity assays, so direct comparisons between studies must take into account not only the form of the enzyme (NS3h vs NS3) but also the specific genotype.[26] Furthermore, NS3 activity is modulated by a cofactor, NS4A, which can stimulate unwinding activity,[27,28] further complicating any direct comparison of binding studies.

Like most helicases, NS3 requires a ssDNA overhang to rapidly initiate unwinding of DNA. The length of the ssDNA overhang can be varied to accommodate more than one molecule of NS3, resulting in an increased level of unwinding, as was shown for the NS3 helicase domain.[24] NS3 is known to bind to ssDNA with a site size of 8 nt,[29] which is consistent with the reported cocrystal structures.[12−14] DNA unwinding experiments are often conducted in the presence of an enzyme concentration that exceeds the substrate concentration. The number of NS3 molecules bound to a specific DNA substrate prior to initiation of a DNA unwinding experiment can be estimated on the basis of the binding site size and the length of the ssDNA. We wished to directly measure the number of molecules of NS3 bound to a specific DNA substrate, so a DNA footprinting assay was applied using $KMnO_4$, which can react with thymidine residues at the C5 and C6 positions.[25,30] After reaction with $KMnO_4$, treatment of the DNA with piperidine results in a cascade of reactions leading to cleavage of the DNA backbone, which can be visualized after separating different sized DNA fragments by gel electrophoresis. Thymidine residues that are exposed, such as in ssDNA, are highly reactive, whereas residues in dsDNA are much less reactive because the site of reaction is sterically shielded. Additionally, protein binding might sequester thymidine residues, which may alter reactivity, depending on whether C5 and C6 are facing the protein or the solvent.

NS3 was incubated with a biotin-labeled oligonucleotide consisting of 23 thymidines, a biotin-labeled spacer, and a 5′-

dx.doi.org/10.1021/bi300654v | Biochemistry 2012, 51, 7596−7607

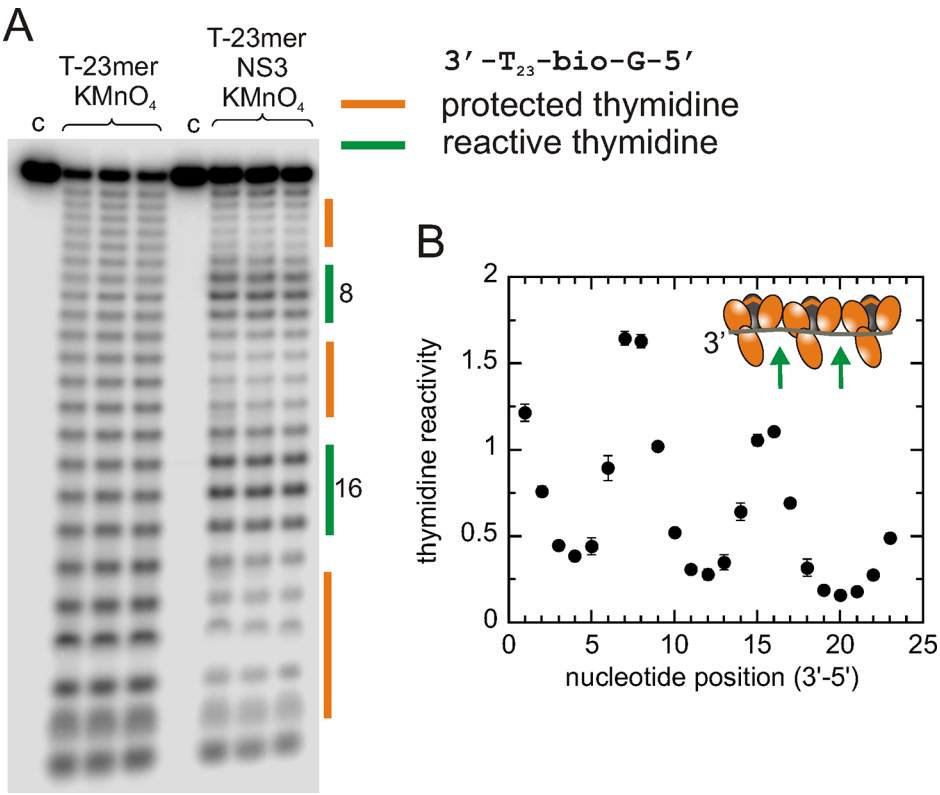

Figure 1. $KMnO_4$ footprinting reveals binding of NS3 to ssDNA with an 8 nt site size. (A) ssDNA substrate consisting of 23 thymidine residues, a biotin-labeled analogue, and a 5′-guanine residue treated with $KMnO_4$ in the presence or absence of NS3. DNA was isolated on streptavidin beads and treated with piperidine, followed by extensive washing prior to separation on a 20% denaturing polyacrylamide gel. In the presence of NS3, regions of low reactivity and high reactivity were observed as indicated by the orange and green bars. Three regions of protection and two regions of high reactivity are indicated by the orange and green bars, respectively. (B) Quantitation of the radioactivity in each band in the presence of NS3 compared to the radioactivity in the absence of NS3 to determine the thymidine reactivity. Each point in the graph is the average of three independent experiments, and error bars reflect the standard deviation from the average. The plot reveals two regions of high reactivity separated by 8 nt. A model showing three molecules of NS3 bound to the oligonucleotide is shown in the inset with arrows indicating sites of high thymidine reactivity. Error bars represent the standard deviation from three experiments.

guanine followed by treatment with $KMnO_4$ (Figure 1). In the absence of NS3, uniform reactivity was observed for all of the thymidine residues (Figure 1A). In the presence of NS3, the polyacrylamide gel revealed a distinct pattern of protection and reactivity. The residues at the 3′-end were reactive; however, positions 3−5 were protected. The bases at positions 7 and 8 exhibited a high level of reactivity. A second region of protection was followed by another region of reactivity at positions 15 and 16. The results were quantified by determining the amount of radioactivity in each band and dividing it by the sum total of radioactivity in the lane to determine the fraction of DNA in each band. The fraction of radioactivity in each band in the presence of NS3 was divided by the fraction of radioactivity in the corresponding band in the absence of NS3 to determine the relative reactivity of each thymidine toward $KMnO_4$. The average of three independent values was plotted for each thymidine position (Figure 1B). The resulting graph indicates that three molecules of NS3 are bound to the oligonucleotide (Figure 1B, inset), which is consistent with the binding site size for NS3 of 7−8 nt based on the crystal structures of the NS3 helicase domain in the presence of ssDNA.[12] The fact that the crystal structure of NS3 indicates 5−6 nt in the binding site whereas the pattern of reactivity repeats every 7−8 nt suggests that the NS3 molecules are packed closely together on the ssDNA. The sites of high reactivity appear to be located between adjacent NS3 molecules as depicted in the inset model showing NS3 bound to the ssDNA.

NS3 Binds to the ssDNA and dsDNA Regions of a Partial Duplex DNA Substrate. DNA unwinding experiments are typically performed using substrates containing a ssDNA overhang. Binding of NS3 to a DNA substrate containing a 3′-overhang has been proposed to result in melting of a few base pairs in the duplex.[20] We examined this possibility using the footprinting reaction, which can report on melted regions of DNA. A partial duplex DNA substrate was prepared containing thymidine residues at each position in the ssDNA region and at every other position in the dsDNA (Figure 2). Treatment of the DNA alone with $KMnO_4$ resulted in a clear pattern of high reactivity in the ssDNA region but little reactivity in the dsDNA region as expected (Figure 2A). Incubation of the DNA (10 nM) with NS3 (500 nM) followed by treatment with $KMnO_4$ led to a distinct pattern of reactivity in the ssDNA region that was similar to that observed in Figure 1, a peak of reactivity at position 8, flanked by two regions of protection (Figure 2B). Reactivity increases near the ssDNA−dsDNA junction at position 15, indicating that two molecules of NS3 are bound to the ssDNA portion of the substrate. This result provides direct evidence that under conditions of excess enzyme concentration relative to DNA, more than one molecule of NS3 is positioned on a 15 nt DNA substrate.

dx.doi.org/10.1021/bi300654v | *Biochemistry* 2012, 51, 7596−7607

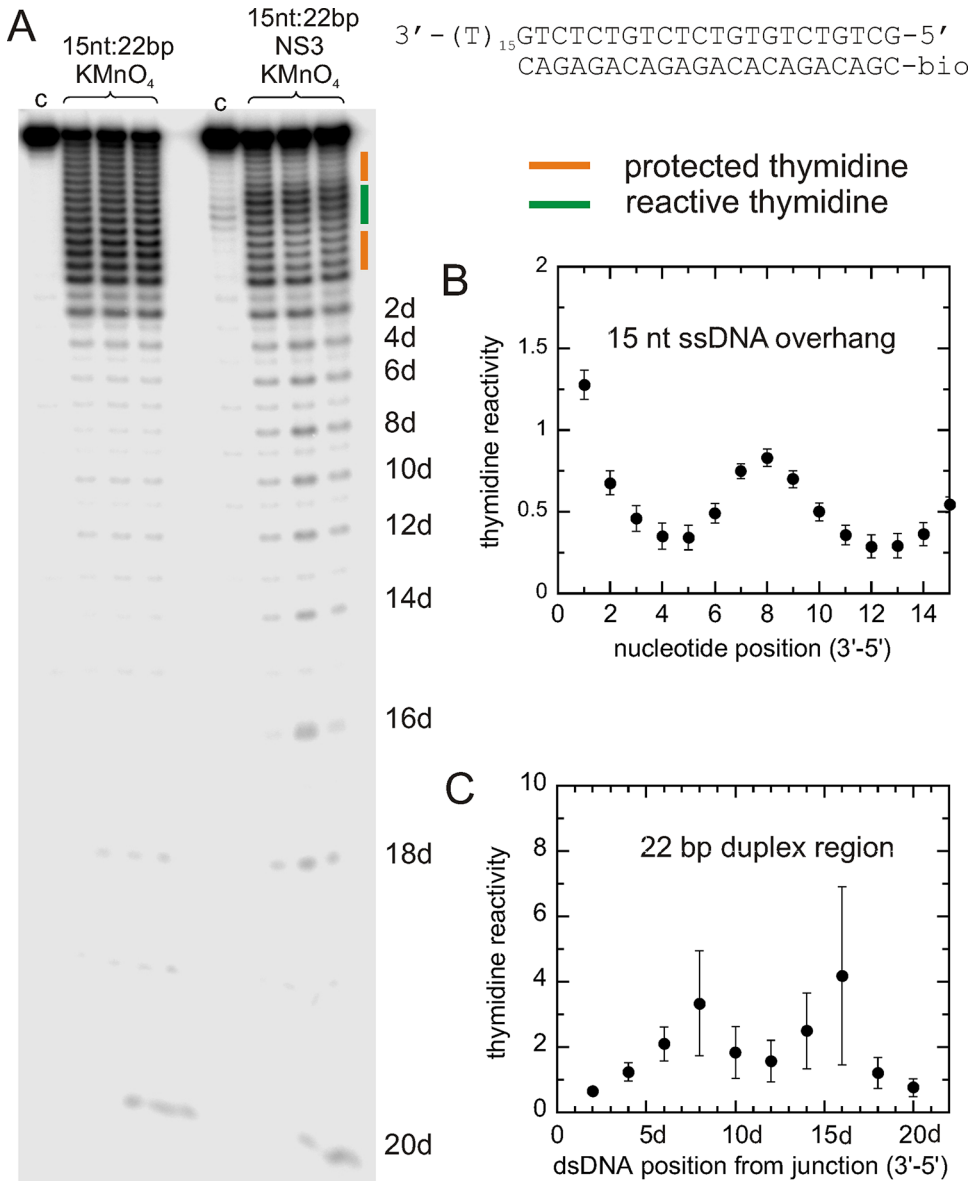

Figure 2. Footprinting with $KMnO_4$ reveals binding of NS3 to the ssDNA and dsDNA regions of a partial duplex DNA substrate. A DNA substrate was designed so that each base in the single-stranded region and every other base in the duplex region was thymidine. A complementary 22mer was hybridized to the thymidine strand to produce a 15 nt, 22 bp DNA substrate. (A) Substrate DNA (10 nM) was incubated in the presence or absence of NS3 (500 nM) for 9 min at 37 °C, followed by reaction with $KMnO_4$. DNA was captured on streptavidin beads followed by treatment with piperidine, and separation on a 20% denaturing polyacrylamide gel. All of the residues in the single-stranded overhang are highly reactive toward $KMnO_4$. Bands corresponding to the thymidine residues in the duplex region are numbered along the right side of the gel and generally exhibit much lower reactivity toward $KMnO_4$. Thymidine residues that are protected or show increased reactivity in the presence of NS3 are indicated by the orange or green bands, respectively. DNA in lanes marked with the letter c was not treated with $KMnO_4$. (B) Thymidine reactivity in the presence of NS3 divided by the reactivity in the absence of NS3 to determine the effect of binding of NS3 to the DNA at each thymidine position. The pattern of reactivity in the ssDNA exhibits a region of high reactivity at position 8 flanked by two regions of protection. (C) Relative reactivity of each thymidine in the duplex region. Two regions of high reactivity are observed at positions 23 and 31, indicating that NS3 binds to the entire length of the partial duplex substrate. Error bars represent the standard deviation from three experiments.

Interestingly, the thymidine residues in the duplex portion of the substrate exhibited much higher reactivity toward $KMnO_4$ in the presence of NS3 than in its absence (Figure 2A). Radioactivity in these bands was quantified, and the reactivity for each position was plotted (Figure 2C; positions are designated by the letter d for duplex). The relative reactivity of thymidines in the duplex region increases much more than in the ssDNA regions because the reactivity in the absence of NS3 is very low. The pattern of reactivity and protection was strikingly similar to that observed in the ssDNA. Two regions of high reactivity centered on positions 8d and 16d were flanked by regions of lower reactivity. Further, the pattern of protection and reactivity in the duplex was an extension of the pattern that started on the single-stranded DNA, with regions of high reactivity being separated by approximately 7−8 nt beginning at the 3′-end.

The reactivity was examined using a DNA substrate that was the same length as in Figure 2, but the thymidine residues were placed into the displaced strand, rather than the tracking strand (Figure 3A). The thymidine reactivity was plotted for the

dx.doi.org/10.1021/bi300654v | *Biochemistry* 2012, 51, 7596−7607

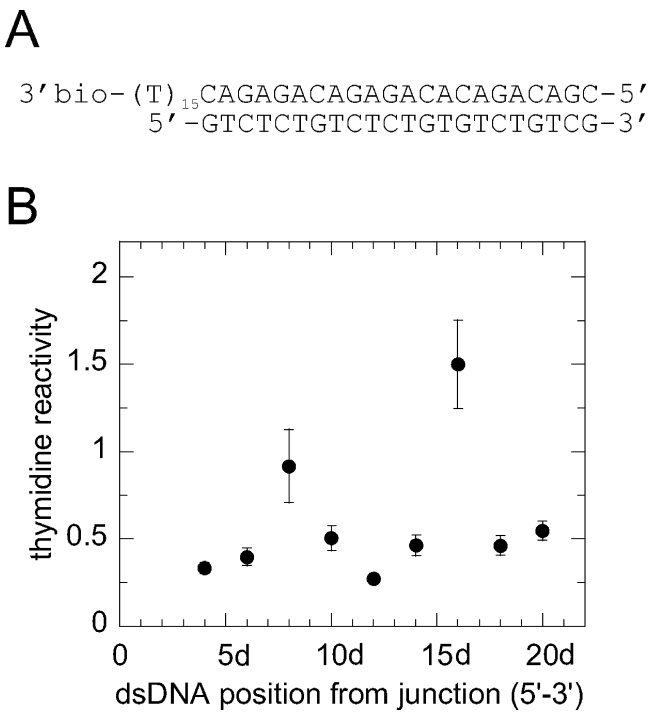

Figure 3. Footprinting of the displaced strand provides a pattern similar to that of the tracking strand. (A) A DNA substrate was prepared with 15 nt of ssDNA and 22 bp, but the sequence contained thymidine residues at every other position in the displaced strand of the duplex region (15 nt, 22 bp T). (B) Permanganate footprinting was performed as described, and the resulting thymidine reactivity is plotted for the displaced strand. The thymidine residues are numbered from the ssDNA–dsDNA junction (the 5′-end of the displaced strand). The reactivity pattern exhibited peaks at positions 8d and 16d, which corresponds to the reactivity pattern observed for the tracking strand as shown in Figure 2.

duplex region by numbering each position from the ssDNA–dsDNA junction. The pattern of reactivity matched closely that shown for the tracking strand, with peaks of reactivity at positions 8d and 16d (Figure 3B).

The appearance of a footprinting pattern in the duplex region led us to examine a longer duplex substrate containing 30 bp. The ssDNA overhang exhibited a familiar pattern like those of the other substrates (Figure 4), and the duplex region exhibited a strong footprinting pattern, especially near the ssDNA–dsDNA junction (Figure 4B). The highest thymidine reactivity within the duplex occurred at position 8d, which is 8 bp from the ssDNA–dsDNA junction. This result suggests that at least one molecule of NS3 is bound within the duplex region. The pattern of reactivity continues within the duplex, exhibiting additional reactivity peaks at positions 16d and 24d. Hence, the reactivity pattern repeats every 8 bp.

It is possible that NS3 melts the duplex by sequestering ssDNA formed because of thermal fraying. However, control experiments in the absence of ATP indicated that only 3% of the 22 bp substrate was separated during a 10 min incubation (Figure 1 of the Supporting Information). No melting was observed in control experiments with the 30 bp substrate (not shown). Therefore, the increased reactivity of the duplex region toward $KMnO_4$ is not due to complete separation of the duplex upon NS3 binding. Rather, the increased reactivity is likely due to partial melting that leads to greater accessibility of the $KMnO_4$ for the C5 and C6 atoms of thymidine residues in the

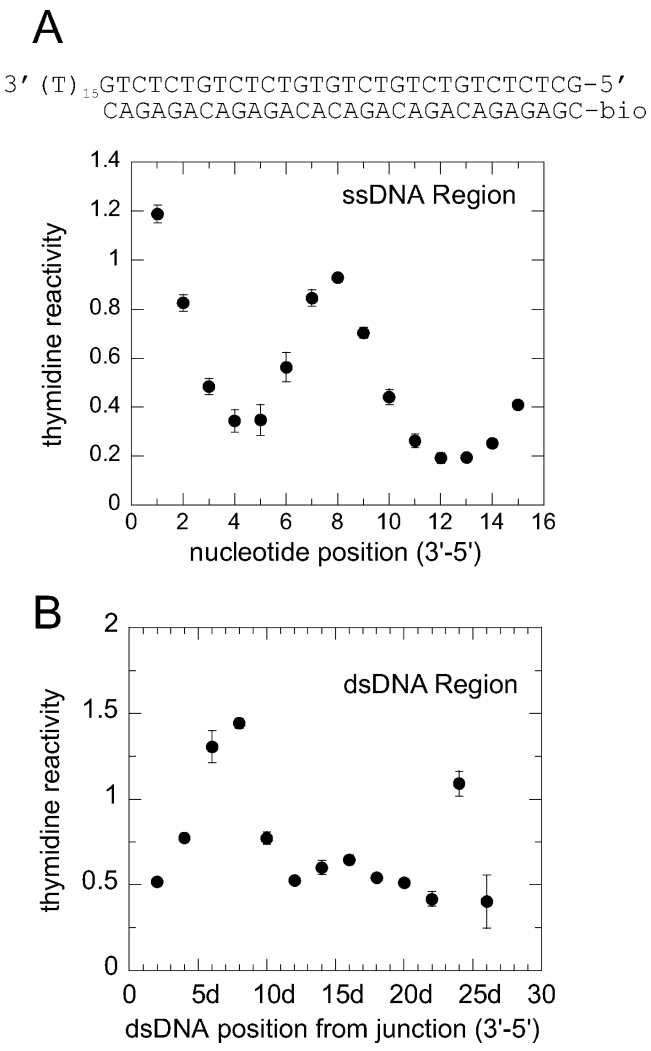

Figure 4. $KMnO_4$ footprinting of NS3 bound to a 15 nt, 30 bp partial duplex. (A) A complementary 30mer was hybridized to the thymidine strand to produce a 15 nt, 30 bp DNA substrate. Substrate DNA (10 nM) was incubated in the presence or absence of NS3 (500 nM) for 9 min at 37 °C, followed by reaction with $KMnO_4$. Thymidine reactivity was determined as described. The pattern of reactivity in the ssDNA region is similar to that observed with the previous substrates, exhibiting a region of high reactivity at position 8 flanked by two regions of protection. (B) Relative reactivity of each thymidine in the duplex region with positions relative to the ssDNA–dsDNA junction. Three regions of high reactivity are observed at positions 8d, 16d, and 24d, indicating that NS3 binds to the entire length of the partial duplex substrate. Error bars represent the standard deviation from three experiments.

duplex region. NS3 appears to be capable of binding to the dsDNA and readily capturing the ssDNA at the junction.

NS3 Binding to Blunt-Ended dsDNA. A blunt-ended 30mer duplex was prepared (Table 1) and examined for binding by $KMnO_4$ footprinting (Figure 5A). The reactivity pattern indicated some binding to the duplex, perhaps because of fraying at the ends (Figure 5B). Hence, NS3 is readily capable of capturing DNA at the ends of the duplex as depicted in the diagram in Figure 5C. Reactivity within the interior of the blunt-ended duplex was less evident compared to that in the substrates that contained a ssDNA overhang.

Increasing the Length of the ssDNA Overhang Shifts the Pattern of Reactivity in the ssDNA. The thymidine

dx.doi.org/10.1021/bi300654v | *Biochemistry* 2012, 51, 7596–7607

Table 1. DNA Sequences Used for $KMnO_4$ Footprinting[a]

3' (T15)-GTC TCT GTC TCT GTG TCT GTC G-5' 5′-CAG AGA CAG AGA CAC AGA CAG C-bio-3′	15nt:22bp
3' (T19)-GTC TCT GTC TCT GTG TCT GTC G-5' 5′-CAG AGA CAG AGA CAC AGA CAG C-bio-3′	19nt:22bp
3′(T15)-GTC TCT GTC TCT GTG TCT GTC TGT CTC TCG-5′ 5′-CAG AGA CAG AGA CAC AGA CAG ACA GAG AGC-bio-3′	15nt:30bp
3'-bio-(T15)-CAG AGA CAG AGA CAC AGA CAG C-5' 5'-GTC TCT GTC TCT GTG TCT GTC G-3'	15nt:22bpT

[a]The 30mer duplex was derived from the 15 nt, 30 bp sequence by removing the ssDNA.

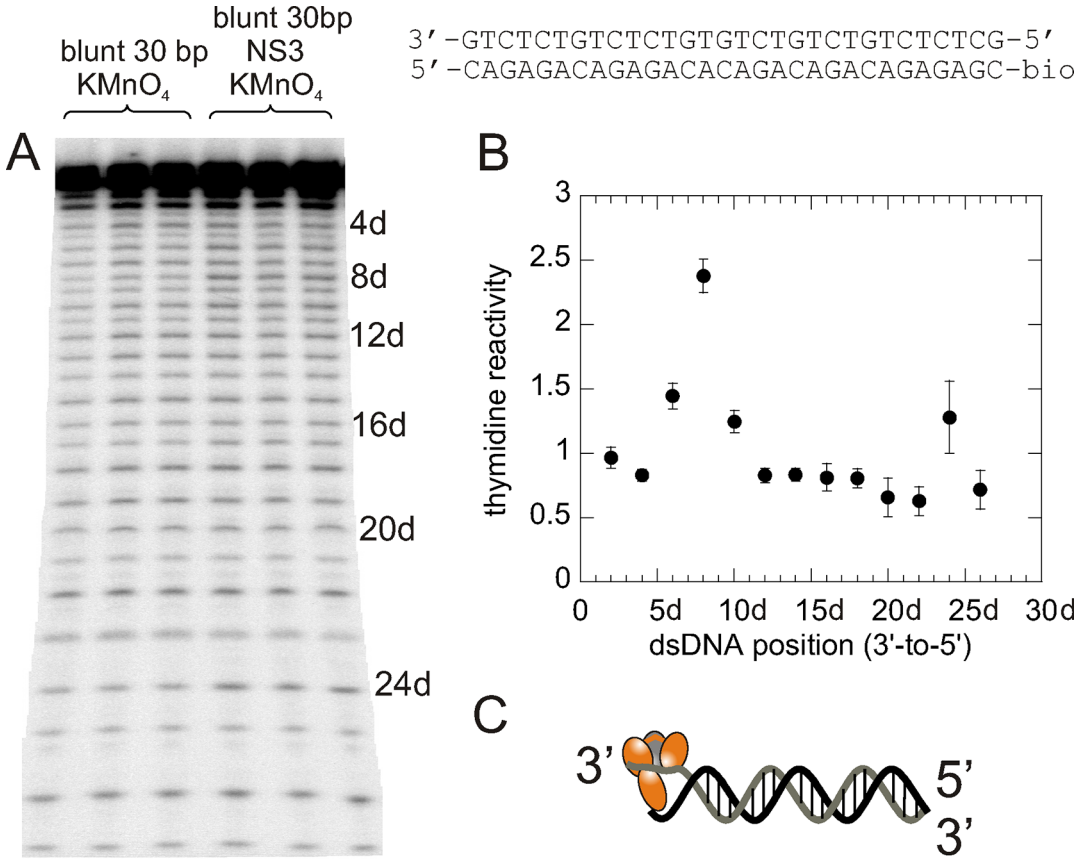

Figure 5. $KMnO_4$ footprinting reveals NS3 binding to the ends of a blunt-end duplex 30mer. (A) A blunt-ended 30mer DNA substrate (10 nM) was prepared containing a thymidine residue at every other position in the radiolabeled strand. Permanganate footprinting was performed as described in the absence or presence of NS3 (500 nM). Numbers to the right of the gel indicate the position from the 3′-end of the strand containing thymidine. (B) Plot of the relative thymidine reactivity in the presence of NS3. The thymidine reactivity pattern exhibited a peak at position 8d and a minor peak at position 24d. (C) Model for binding of NS3 to the end of the duplex.

reactivity exhibited a repeating pattern of ~8 bp, consistent with the site size of NS3. To further examine the pattern of reactivity, a partial duplex substrate was prepared in which the ssDNA overhang was increased in length by 4 nt from 15 to 19 nt. The duplex region remained the same at 22 bp with a thymidine residue occupying every other position (Table 1). $KMnO_4$ footprinting resulted in a peak of reactivity at positions 7 and 8 in the ssDNA region (Figure 6A), similar to that which was observed with the 15 nt substrate (Figures 1B and 2B). A minor peak of reactivity in the 19 nt ssDNA was observed at position 15 but was not clearly defined. Hence, the reactivity pattern in the ssDNA was shifted by 4 nt, consistent with NS3 binding to the 3′-end of the ssDNA.

The reactivity pattern in the duplex region exhibited a peak at position 6d (Figure 6B). This peak is shifted compared with the peak of reactivity observed for the 15 nt, 22 bp substrate (Figure 2B) or the 15 nt, 30 bp substrate (Figure 4B), which occurred at position 8d. The resolution of the reactivity pattern is limited to 2 bp, so the shift in the peak is 1−2 bp in the duplex region compared to the other substrates. In contrast, the initial reactivity pattern of the ssDNA region of the 19 nt, 22 bp substrate is similar to that of the 15 nt, 22 bp substrate, exhibiting a shift of 4 nt. The reactivity pattern in the remainder of the ssDNA is less well-defined (Figure 6A). The reactivity pattern in the duplex region of the 19 nt, 22 bp substrate is similar to that observed for the other dsDNA regions. The fact that the pattern in the duplex region exhibits only a small shift in the position of the reactivity peak supports the conclusion that NS3 prefers to bind to the ssDNA−dsDNA junction.

dx.doi.org/10.1021/bi300654v | *Biochemistry* 2012, 51, 7596−7607

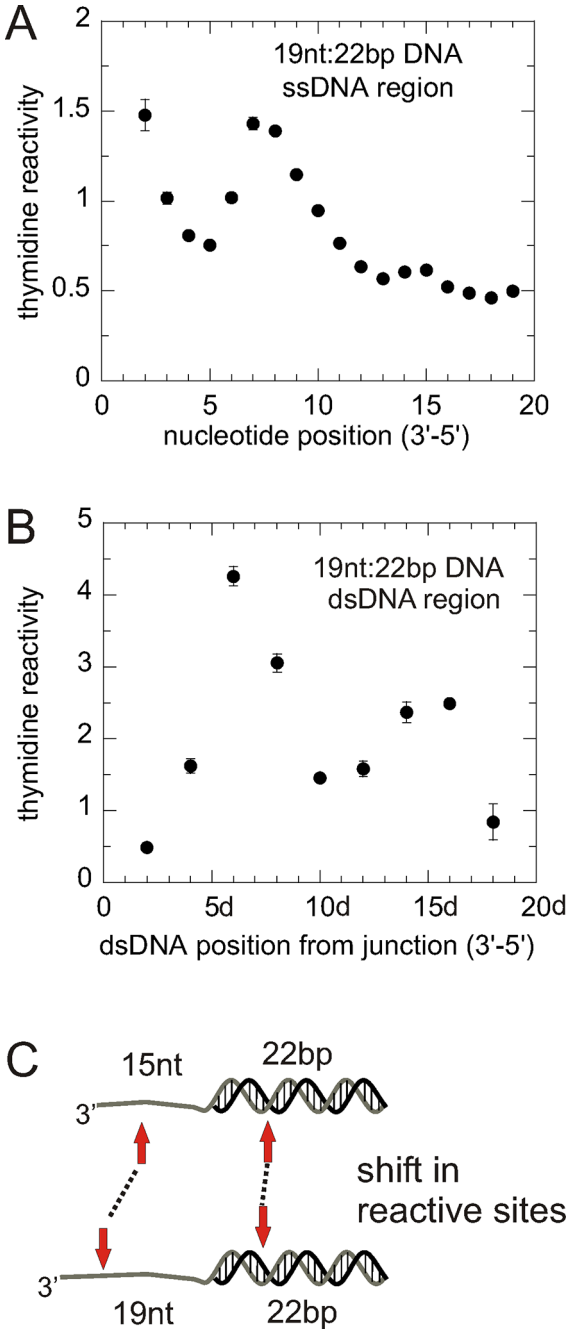

Figure 6. Increasing the length of the ssDNA reveals a shift in the position of $KMnO_4$ reactivity toward the 3′-end of the ssDNA. (A) A substrate was designed such that the ssDNA overhang contained 19 nt and 22 bp. $KMnO_4$ footprinting was performed in the absence or presence of NS3 (500 nM) as described. The pattern of thymidine reactivity in the ssDNA portion of the substrate exhibited a peak at positions 7 and 8 and a minor peak at position 15. (B) The pattern of thymidine reactivity in the duplex region exhibited a peak at position 6d and position 14d. (C) Diagram showing how the reactive sites for the 15 nt, 22 bp substrate compare to those for the 19 nt, 22 bp substrate. The major peak in reactivity in the ssDNA region is shifted by 4 nt. The major peak in reactivity in the dsDNA is shifted by 1−2 bp.

NS3 Binds to the ssDNA Rapidly and Then More Slowly Binds to the dsDNA Region. Binding of NS3 to the single-stranded and duplex regions of the substrate was examined by probing with $KMnO_4$ as a function of increasing incubation times. The gel image clearly indicates that the ssDNA region is bound very rapidly because the protection pattern appears in the first 30 s (Figure 7A). However, the increased reactivity in the duplex appears more slowly. The reactivity of the DNA toward $KMnO_4$ was determined as described above and plotted for thymidine residues in the ssDNA region (Figure 7B) or in the dsDNA region (Figure 7C) as a function of incubation time. The reactivity in the ssDNA region exhibits little or no change during the 9 min incubation. However, the reactivity in the duplex region increases, as is shown for selected thymidine positions in Figure 7C. The increase in reactivity is especially noted at thymidine residues in the interior duplex region such as those at positions 8d and 16d. The increase in reactivity is a measure of the stronger propensity for $KMnO_4$ to react with thymidine residues. The reactivity of $KMnO_4$ within the duplex region of the DNA does not reflect complete strand separation but instead must reflect a transition in the local structure of the duplex DNA that leads to greater reactivity of thymidine with $KMnO_4$. We conclude that the dsDNA is partially melted or untwisted to some degree, thereby exposing the reactive sites of thymidine to $KMnO_4$.

NS3 Binds the Duplex Region Even at Low Concentrations Relative to That of the DNA Substrate. Binding of NS3 to the 15 nt, 22 bp substrate was investigated by varying the enzyme concentration. NS3 (50, 100, 250, 500, or 1000 nM) was incubated for 9 min with DNA (10 nM) followed by reaction with $KMnO_4$ for 5 s. Each DNA molecule contains five binding sites for NS3 based on a 7−8 nt binding site size, so that 10 nM substrate can bind 50 nM NS3 (two sites in the ssDNA region and three possible sites in the duplex region). Comparison of the reactivity in the ssDNA region (Figure 8A) with the reactivity in the dsDNA region (Figure 8B) indicates that the pattern of protection and reactivity appears within the duplex region of the substrate even at the lowest concentration of NS3 (see the expanded view in Figure 8C). The reactivity peak is not clearly observed at the lowest NS3 concentration for the ssDNA region (Figure 8A). This may be due to random binding of NS3 to ssDNA at a low NS3 concentration, which might result in general protection of the ssDNA. However, the pattern of protection is observed in the dsDNA region, which further supports a preference for binding to the ssDNA−dsDNA junction. Hence, multiple molecules of NS3 bind along the DNA, even when the concentration of NS3 is similar to the concentration of available binding sites. This result also supports the conclusion that the majority of the enzyme is available for binding to the DNA, as previously reported.[17,31]

■ DISCUSSION

In a description of the mechanism of helicases, it is useful to distinguish between translocation on ssDNA and melting of duplex DNA. The two processes are clearly related and may indeed occur in the same step in the overall mechanism for DNA unwinding for some helicases. However, there are mechanisms in which translocation and melting are distinguishable, and different experimental methods can report on different aspects of the mechanism. The reported structures of NS3 clearly illustrate the path of the ssDNA through the active site in the enzyme.[12−14] ATP binding causes closure of the two RecA domains, which is coupled to directionally biased movement through the "ratchetlike" interactions between amino acid residues such as the base stacking interaction between Trp501 and ssDNA. Translocation on ssDNA or

dx.doi.org/10.1021/bi300654v | Biochemistry 2012, 51, 7596−7607

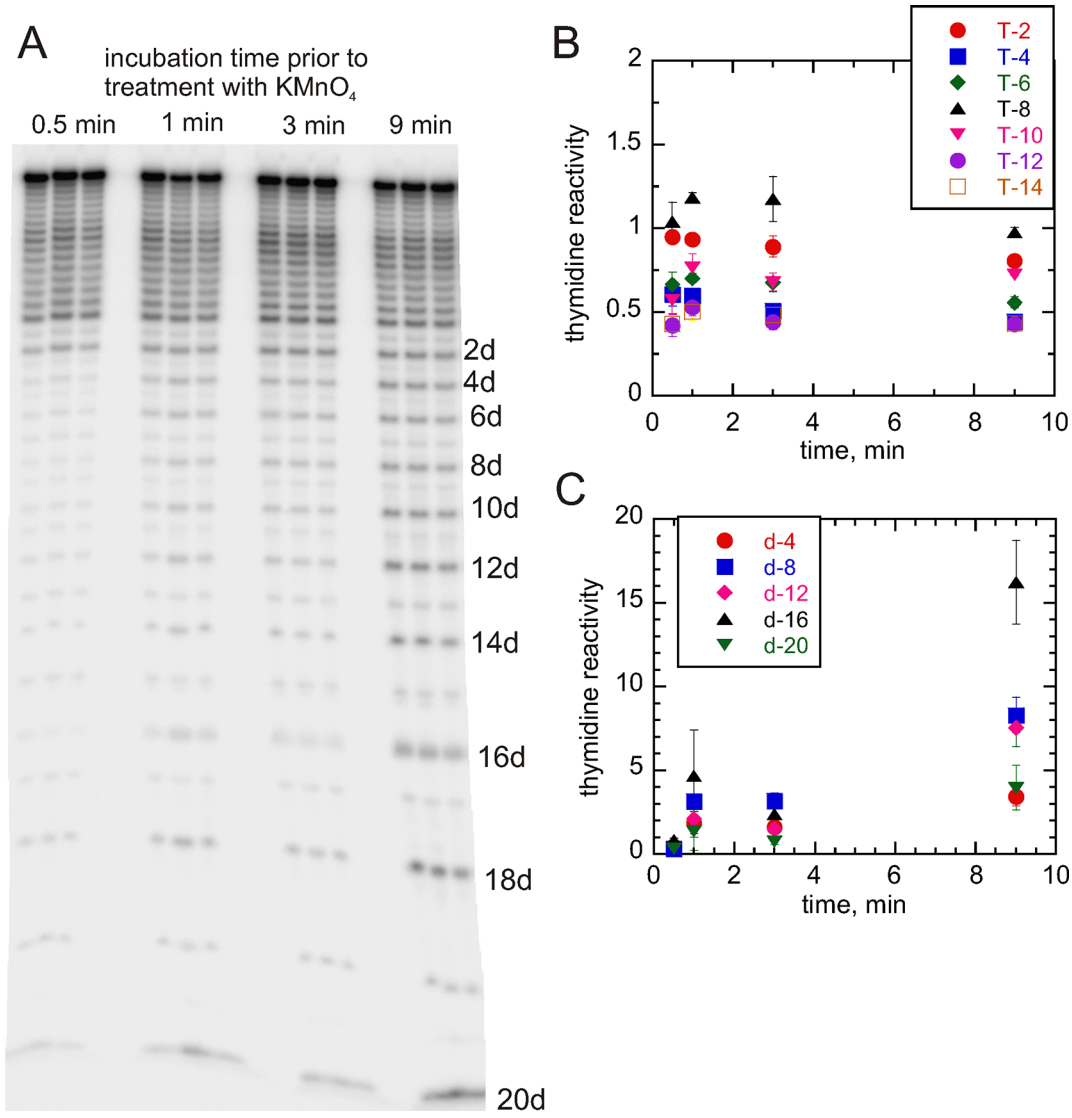

Figure 7. Thymidine reactivity with $KMnO_4$ determined as a function of the time of incubation of NS3 with DNA. (A) NS3 was incubated with the 15 nt, 22 bp DNA for 0.5, 1.0, 3.0, or 9.0 min at 37 °C, followed by reaction with $KMnO_4$ for 5 s. DNA was captured on streptavidin beads and treated with piperidine, followed by separation on a 20%, denaturing polyacrylamide gel and visualization using a PhosphorImager. Thymidine positions in the duplex region are numbered to the right of the gel. (B) Thymidine reactivity toward $KMnO_4$ for each band in the ssDNA region determined as described in Materials and Methods. The reactivity was plotted vs time and is shown for every other thymidine position in the ssDNA region, as depicted in the legend on the plot. (C) Reactivity of thymidine toward $KMnO_4$ for selected positions in the dsDNA region plotted vs time. The reactivity generally increases as a function of time in the duplex region.

ssRNA is believed to occur in 1 nt steps per each ATP molecule hydrolyzed, although the coupling efficiency varies between specific forms of the enzyme.[16,27]

The number of base pairs that can be melted for each translocation step is under active debate. A 9 bp RNA substrate was designed that could be melted by NS3 in a single substep, as indicated by the lack of a lag phase and the 90% amplitude observed during single-cycle unwinding.[32] Although the RNA duplex contained 9 bp, some of the base pairs may melt spontaneously because of thermal fraying, so the specific number of base pairs melted in a single cycle is difficult to reveal in an ensemble experiment. Single-molecule Förster resonance energy transfer (smFRET)[33] and structural[13] studies have suggested a "springlike" motion whereby domains 1 and 2 move by 1 nt increments while domain 3 engages the nucleic acid more tightly through interaction with amino acid residue Trp501. The relative movement of the domains is proposed to build up strain that is released after three translocation steps leading to unzipping of 3 bp. An alternative explanation for melting was provided by studies in which single-molecule laser tweezers were used to measure step sizes of 0.5−3 bp.[34] The explanation provided for the variable melting step was based on a proposed second site on the surface of NS3 for binding to the displaced strand. Translocation of NS3 on the tracking strand by 1 nt steps was proposed, but release of the displaced strand was suggested to occur in a manner that does not correlate precisely with translocation, giving rise to the appearance of variable step sizes for base pair melting. Identification of the residues responsible for binding to the displaced strand may help delineate the differences in the proposed mechanisms.[35]

A Brownian motor mechanism has also been proposed for translocation and unwinding by the NS3 helicase domain (NS3h).[20] In this mechanism, two states of binding to DNA, weak and tight, are modulated by ATP binding. In the weak

dx.doi.org/10.1021/bi300654v | *Biochemistry* 2012, 51, 7596−7607

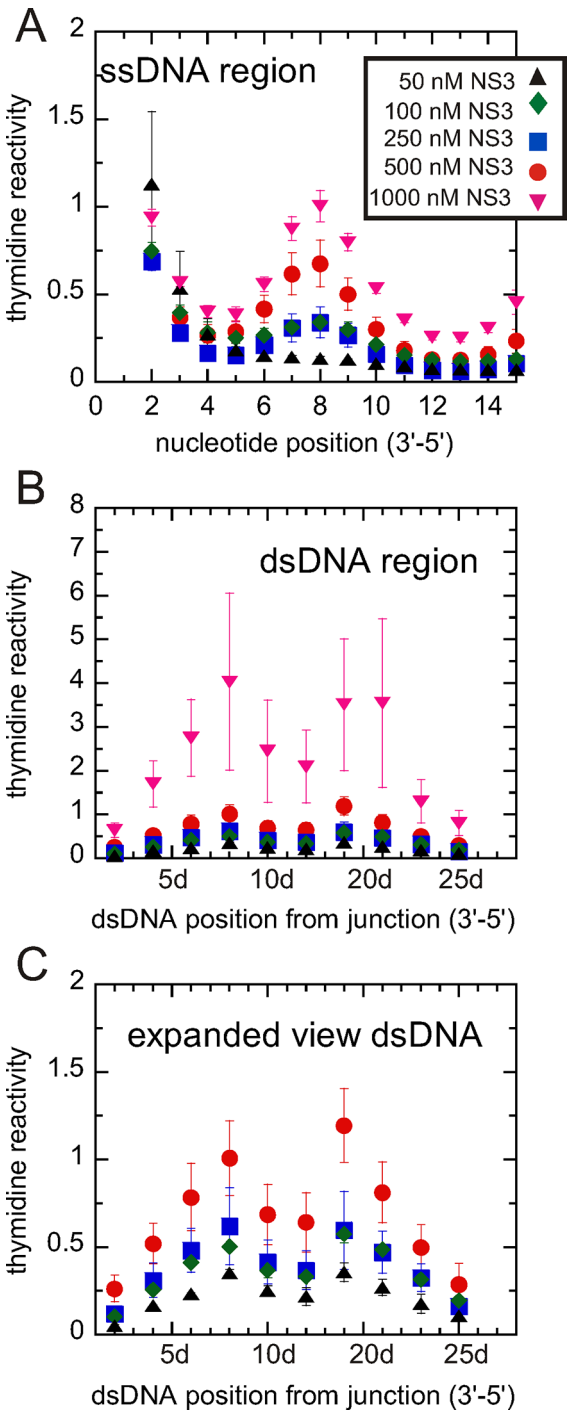

Figure 8. $KMnO_4$ footprinting pattern that is similar over a range of NS3 concentrations. Increasing concentrations of NS3 [50 nM (black triangles), 100 nM (green diamonds), 250 nM (blue squares), 500 nM (red circles), and 1000 nM (magenta triangles)] were incubated with the 15 nt, 22 bp DNA (10 nM) for 9 min followed by footprinting with $KMnO_4$. The reactivity of thymidine with $KMnO_4$ is plotted for each position in the ssDNA region (A) or in the dsDNA region (B). (C) Expanded view of the dsDNA region. The pattern of protection and reactivity of thymidine with $KMnO_4$ in the dsDNA region can be observed even at 50 nM NS3 (black triangles), at which the concentration of available DNA binding sites is equal to the concentration of NS3.

ATP-bound state, NS3h diffuses along the DNA. Hydrolysis and release of the cofactor lead to a tight binding state, and directional movement occurs as a result of an asymmetric "sawtooth" energy profile. On the basis of the ongoing discussion for the mechanism of unwinding by NS3, this area of study will likely remain an active area of investigation and the enzyme will likely continue to serve as a model system for other helicases.

A Model for Binding of NS3 to ssDNA–dsDNA Junction. In this report, we have utilized a method that has the potential to report on the position of the helicase on the DNA as well as the status of the DNA. $KMnO_4$ reacts with thymidine residues more rapidly than other bases, with the rate of reaction being dependent on the exposure of the C5 and C6 atoms (i.e., single-stranded vs double-stranded). This approach has been used extensively to examine interactions between RNA polymerase holoenzyme and promoters during transcription initiation.[36] Some investigators have applied this approach to study the binding of the helicase to DNA.[37,38] One study showed a specific role for DNA melting as a result of helicase binding for the RecBCD enzyme. Melting of 6 bp of dsDNA upon binding of RecBCD in the presence of Mg^{2+} allows the enzyme to overcome a kinetic barrier to begin the rapid unwinding of DNA.[38]

Our experiments were designed to determine the number and position of NS3 molecules bound to a DNA substrate prior to initiation of an unwinding reaction. The number of molecules bound to the ssDNA substrate clearly correlated directly to the binding site size of the enzyme, which is 7–8 nt. Surprisingly, NS3 was found to interact with the duplex portion of the substrate, producing a reactivity pattern with $KMnO_4$ that extended the pattern observed on ssDNA. Binding to the ssDNA occurs very rapidly (<15 s), whereas binding to the duplex occurs more slowly, but within the first 5 min of incubation under the conditions used here (Figure 7). This result indicates that interaction of NS3 with dsDNA leads to partial melting of the duplex, which exposes some thymidine residues for reaction with $KMnO_4$. Alternatively, NS3 is poised to capture ssDNA because of thermal fraying, perhaps as a result of a preferential interaction at the ssDNA–dsDNA junction. These results are consistent with a previous report indicating that NS3 binds relatively well to dsDNA (K_D value between 10 and 20 nM).[17] The results also suggest that multiple molecules of NS3 are poised to participate in the unwinding reaction when the NS3 concentration is in excess of the DNA substrate concentration. A model for the interaction between NS3 and the 15 nt, 22 bp substrate is shown in Figure 9. Initial binding occurs with two NS3 molecules along the ssDNA region. Additional molecules of NS3 then bind more slowly to the dsDNA adjacent to those already bound to the ssDNA. Binding of NS3 to the duplex may predispose the DNA for melting in the presence of ATP. Binding of dsDNA does not lead to the complete separation of the duplex initially but instead causes some degree of untwisting, or partial melting, which increases the reactivity of thymidine residues with $KMnO_4$.

Previous work indicated that unwinding by NS3 was highly sensitive to the structure of the duplex.[39] Structural alteration of the displaced strand led to slower unwinding, suggesting that NS3 interacts with the displaced strand. More recent reports using single-molecule experiments[40] also indicated that NS3 is highly sensitive to the structure of the duplex region of a substrate. The results reported here using DNA footprinting clearly show interaction of NS3 with the duplex region, which provides an explanation for why this enzyme is sensitive to the

dx.doi.org/10.1021/bi300654v | *Biochemistry* 2012, 51, 7596–7607

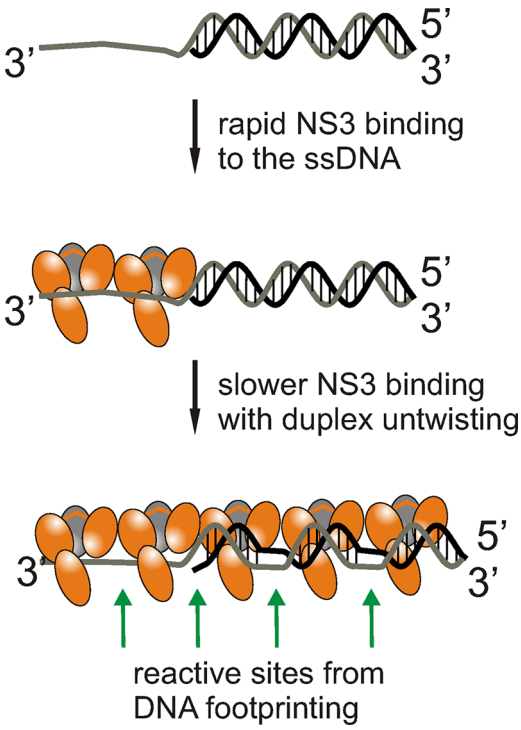

Figure 9. Model for binding of NS3 to a partial duplex DNA substrate. Diagram showing NS3 binding to the 15 nt, 22 bp substrate. The model takes into account the data from the DNA footprinting experiments with $KMnO_4$ that indicate that 7−8 nt (or bp) is bound per NS3 molecule. Initial binding of two molecules of NS3 occurs on the ssDNA overhang, followed by slower binding to the duplex. Binding to the duplex region results in changes in DNA conformation that increase the reactivity of thymidine with $KMnO_4$, consistent with untwisting of the duplex.

duplex structure. The reactivity of the duplex region with $KMnO_4$ in the presence of NS3 indicates that the duplex is actively engaged by the enzyme. Under conditions in which the enzyme concentration greatly exceeds the substrate concentration, the interaction between NS3 and duplex DNA may be facilitated by the propensity of NS3 to form oligomeric structures.[17,22] In such a mechanism, binding of NS3 to the ssDNA region of a partial duplex substrate could help recruit additional molecules to the duplex region through protein−protein interactions.

One of the important implications of these data is that the number of molecules of NS3 bound to the substrate is not defined exclusively by the length of the ssDNA overhang. The 15 nt ssDNA overhang can clearly bind two molecules of NS3, as shown by the DNA footprinting patterns. NS3 can also bind within the duplex portion; therefore, more molecules of NS3 may be poised to participate in the unwinding reaction than the number predicted by the length of the ssDNA. Hence, it may not be possible to limit the number of molecules bound to the substrate by simply varying the length of the ssDNA. Additionally, the number of base pairs melted during the unwinding reaction may also be difficult to discern because some base pairs appear to be melted simply because of binding.

NS3 exhibits a very large kinetic step size of ∼16 bp in ensemble experiments[17,21] and 11 bp in single-molecule experiments.[34,40] Mechanisms proposed to account for the large kinetic step size include fast unwinding followed by a slower step that limits the overall appearance of ssDNA. The slow step has recently been proposed to be due to binding of both DNA strands to NS3, with slow release of the displaced strand limiting the rate of processive unwinding.[35] It is possible that the physical basis for the large kinetic step size does not correlate with the rapid unzipping observed in single-molecule experiments. The results from DNA footprinting favor an interaction between NS3 and both strands of the substrate, producing a protein−DNA complex that untwists or partially melts a relatively large region of the dsDNA prior to initiation of ATP-dependent strand separation. If untwisting or partial melting of the dsDNA is necessary for the subsequent unwinding reaction to ensue, then this process may limit the overall rate of unwinding, thereby providing the slow step in the overall kinetic mechanism.

Whether binding of NS3 to DNA has a biological impact on HCV infection remains to be determined. NS3 can affect activities in the nucleus through its interaction with p53,[19] ATM,[41] and SRCAP,[42] all known regulators of gene expression. However, such protein−protein interactions can occur outside the nucleus, thereby altering the localization of nuclear proteins, which can lead to changes in DNA metabolism. NS3 has been detected in the nuclei of patients infected with HCV, but DNA binding in vivo has not been shown explicitly.[18] Regardless of the biological outcomes of NS3 with DNA, understanding the similarities and differences in how NS3 interacts with DNA and RNA is mechanistically valuable, because it is not known exactly how helicases distinguish between the two biological polymers.

■ ASSOCIATED CONTENT

Supporting Information

Control experiments in which the lack of DNA melting was confirmed after prolonged incubation of NS3 with DNA in the absence of ATP (Figure 1). This material is available free of charge via the Internet at http://pubs.acs.org.

■ AUTHOR INFORMATION

Corresponding Author

*Telephone: (501) 686-5244. Fax: (501) 686-8169. E-mail: raneykevind@uams.edu.

Present Addresses

[§]Department of Psychiatry, University of Arkansas for Medical Sciences, Little Rock, AR 72205.

[‖]Department of Pathology, University of Arkansas for Medical Sciences, Little Rock, AR 72205.

Funding

This work was supported by National Institutes of Health (NIH) Grant GM089001 (K.D.R. and C.E.C.), NIH Grant P20 RR-16460 (L. Cornett) from the IDeA Networks of Biomedical Research Excellence (INBRE) Program, and NIH Grant UL1RR029884 (C. Lowery) from the NCATS.

Notes

The authors declare no competing financial interest.

■ ACKNOWLEDGMENTS

We thank Alicia K. Byrd for helpful discussions and comments on the manuscript.

■ ABBREVIATIONS

dsDNA, double-stranded DNA; ssDNA, single-stranded DNA; NA, nucleic acid; NS3, nonstructural protein 3; HCV, hepatitis C virus; SF, superfamily; $KMnO_4$, potassium permanganate;

smFRET, single-molecule Förster resonance energy transfer; nt, nucleotide.

REFERENCES

(1) Lohman, T. M., Tomko, E. J., and Wu, C. G. (2008) Non-hexameric DNA helicases and translocases: Mechanisms and regulation. *Nat. Rev. Mol. Cell Biol. 9*, 391−401.

(2) Patel, S. S., and Donmez, I. (2006) Mechanisms of helicases. *J. Biol. Chem. 281*, 18265−18268.

(3) Pyle, A. M. (2008) Translocation and unwinding mechanisms of RNA and DNA helicases. *Annu. Rev. Biophys. 37*, 317−336.

(4) Singleton, M. R., Dillingham, M. S., and Wigley, D. B. (2007) Structure and mechanism of helicases and nucleic acid translocases. *Annu. Rev. Biochem. 76*, 23−50.

(5) Myong, S., and Ha, T. (2010) Stepwise translocation of nucleic acid motors. *Curr. Opin. Struct. Biol. 20*, 121−127.

(6) Frick, D. N. (2007) The hepatitis C virus NS3 protein: A model RNA helicase and potential drug target. *Curr. Issues Mol. Biol. 9*, 1−20.

(7) Morikawa, K., Lange, C. M., Gouttenoire, J., Meylan, E., Brass, V., Penin, F., and Moradpour, D. (2011) Nonstructural protein 3-4A: The Swiss army knife of hepatitis C virus. *Journal of Viral Hepatisis 18*, 305−315.

(8) Raney, K. D., Sharma, S. D., Moustafa, I. M., and Cameron, C. E. (2010) Hepatitis C virus non-structural protein 3 (HCV NS3): A multifunctional antiviral target. *J. Biol. Chem. 285*, 22725−22731.

(9) Lam, A. M., Rypma, R. S., and Frick, D. N. (2004) Enhanced nucleic acid binding to ATP-bound hepatitis C virus NS3 helicase at low pH activates RNA unwinding. *Nucleic Acids Res. 32*, 4060−4070.

(10) Fairman-Williams, M. E., Guenther, U. P., and Jankowsky, E. (2010) SF1 and SF2 helicases: Family matters. *Curr. Opin. Struct. Biol. 20*, 313−324.

(11) Gorbalenya, A. E., and Koonin, E. V. (1993) Helicases: Amino acid sequence comparisons and structure-function relationships. *Curr. Opin. Struct. Biol. 3*, 419−429.

(12) Kim, J. L., Morgenstern, K. A., Griffith, J. P., Dwyer, M. D., Thomson, J. A., Murcko, M. A., Lin, C., and Caron, P. R. (1998) Hepatitis C virus NS3 RNA helicase domain with a bound oligonucleotide: The crystal structure provides insights into the mode of unwinding. *Structure 6*, 89−100.

(13) Appleby, T. C., Anderson, R., Fedorova, O., Pyle, A. M., Wang, R., Liu, X., Brendza, K. M., and Somoza, J. R. (2011) Visualizing ATP-Dependent RNA Translocation by the NS3 Helicase from HCV. *J. Mol. Biol. 405*, 1139−1153.

(14) Gu, M., and Rice, C. M. (2010) Three conformational snapshots of the hepatitis C virus NS3 helicase reveal a ratchet translocation mechanism. *Proc. Natl. Acad. Sci. U.S.A. 107*, 521−528.

(15) Matlock, D. L., Yeruva, L., Byrd, A. K., Mackintosh, S. G., Langston, C., Brown, C., Cameron, C. E., Fischer, C. J., and Raney, K. D. (2010) Investigation of translocation, DNA unwinding, and protein displacement by NS3h, the helicase domain from the hepatitis C virus helicase. *Biochemistry 49*, 2097−2109.

(16) Rajagopal, V., Gurjar, M., Levin, M. K., and Patel, S. S. (2010) The Protease Domain Increases the Translocation Stepping Efficiency of the Hepatitis C Virus NS3-4A Helicase. *J. Biol. Chem. 285*, 17821−17832.

(17) Tackett, A. J., Chen, Y., Cameron, C. E., and Raney, K. D. (2005) Multiple full-length NS3 molecules are required for optimal unwinding of oligonucleotide DNA in vitro. *J. Biol. Chem. 280*, 10797−10806.

(18) Errington, W., Wardell, A. D., McDonald, S., Goldin, R. D., and McGarvey, M. J. (1999) Subcellular localisation of NS3 in HCV-infected hepatocytes. *J. Med. Virol. 59*, 456−462.

(19) Muramatsu, S., Ishido, S., Fujita, T., Itoh, M., and Hotta, H. (1997) Nuclear localization of the NS3 protein of hepatitis C virus and factors affecting the localization. *J. Virol. 71*, 4954−4961.

(20) Levin, M. K., Gurjar, M., and Patel, S. S. (2005) A Brownian motor mechanism of translocation and strand separation by hepatitis C virus helicase. *Nat. Struct. Mol. Biol. 12*, 429−435.

(21) Serebrov, V., and Pyle, A. M. (2004) Periodic cycles of RNA unwinding and pausing by hepatitis C virus NS3 helicase. *Nature 430*, 476−480.

(22) Sikora, B., Chen, Y., Lichti, C. F., Harrison, M. K., Jennings, T. A., Tang, Y., Tackett, A. J., Jordan, J. B., Sakon, J., Cameron, C. E., and Raney, K. D. (2008) Hepatitis C virus NS3 helicase forms oligomeric structures that exhibit optimal DNA unwinding activity in vitro. *J. Biol. Chem. 283*, 11516−11525.

(23) Ding, S. C., Kohlway, A. S., and Pyle, A. M. (2011) Unmasking the active helicase conformation of nonstructural protein 3 from hepatitis C virus. *J. Virol. 85*, 4343−4353.

(24) Levin, M. K., Wang, Y. H., and Patel, S. S. (2004) The functional interaction of the hepatitis C virus helicase molecules is responsible for unwinding processivity. *J. Biol. Chem. 279*, 26005−26012.

(25) Bui, C. T., Rees, K., and Cotton, R. G. (2003) Permanganate oxidation reactions of DNA: Perspective in biological studies. *Nucleosides, Nucleotides Nucleic Acids 22*, 1835−1855.

(26) Lam, A. M., Keeney, D., Eckert, P. Q., and Frick, D. N. (2003) Hepatitis C virus NS3 ATPases/helicases from different genotypes exhibit variations in enzymatic properties. *J. Virol. 77*, 3950−3961.

(27) Beran, R. K., Lindenbach, B. D., and Pyle, A. M. (2009) The NS4A protein of hepatitis C virus promotes RNA-coupled ATP hydrolysis by the NS3 helicase. *J. Virol. 83*, 3268−3275.

(28) Pang, P. S., Jankowsky, E., Planet, P. J., and Pyle, A. M. (2002) The hepatitis C viral NS3 protein is a processive DNA helicase with cofactor enhanced RNA unwinding. *EMBO J. 21*, 1168−1176.

(29) Levin, M. K., and Patel, S. S. (2002) Helicase from hepatitis C virus, energetics of DNA binding. *J. Biol. Chem. 277*, 29377−29385.

(30) Holstege, F. C., and Timmers, H. T. (1997) Analysis of open complex formation during RNA polymerase II transcription initiation using heteroduplex templates and potassium permanganate probing. *Methods 12*, 203−211.

(31) Jennings, T. A., Mackintosh, S. G., Harrison, M. K., Sikora, D., Sikora, B., Dave, B., Tackett, A. J., Cameron, C. E., and Raney, K. D. (2009) NS3 helicase from the hepatitis C virus can function as a monomer or oligomer depending on enzyme and substrate concentrations. *J. Biol. Chem. 284*, 4806−4814.

(32) Wang, Q., Arnold, J. J., Uchida, A., Raney, K. D., and Cameron, C. E. (2010) Phosphate release contributes to the rate-limiting step for unwinding by an RNA helicase. *Nucleic Acids Res. 38*, 1312−1324.

(33) Myong, S., Bruno, M. M., Pyle, A. M., and Ha, T. (2007) Spring-loaded mechanism of DNA unwinding by hepatitis C virus NS3 helicase. *Science 317*, 513−516.

(34) Cheng, W., Arunajadai, S. G., Moffitt, J. R., Tinoco, I., Jr., and Bustamante, C. (2011) Single-base pair unwinding and asynchronous RNA release by the hepatitis C virus NS3 helicase. *Science 333*, 1746−1749.

(35) Serebrov, V., Beran, R. K., and Pyle, A. M. (2009) Establishing a mechanistic basis for the large kinetic steps of the NS3 helicase. *J. Biol. Chem. 284*, 2512−2521.

(36) Gries, T. J., Kontur, W. S., Capp, M. W., Saecker, R. M., and Record, M. T., Jr. (2010) One-step DNA melting in the RNA polymerase cleft opens the initiation bubble to form an unstable open complex. *Proc. Natl. Acad. Sci. U.S.A. 107*, 10418−10423.

(37) Farah, J. A., and Smith, G. R. (1997) The RecBCD enzyme initiation complex for DNA unwinding: Enzyme positioning and DNA opening. *J. Mol. Biol. 272*, 699−715.

(38) Wong, C. J., and Lohman, T. M. (2008) Kinetic control of Mg^{2+}-dependent melting of duplex DNA ends by *Escherichia coli* RecBC. *J. Mol. Biol. 378*, 761−777.

(39) Tackett, A. J., Wei, L., Cameron, C. E., and Raney, K. D. (2001) Unwinding of nucleic acids by HCV NS3 helicase is sensitive to the structure of the duplex. *Nucleic Acids Res. 29*, 565−572.

(40) Cheng, W., Dumont, S., Tinoco, I., Jr., and Bustamante, C. (2007) NS3 helicase actively separates RNA strands and senses sequence barriers ahead of the opening fork. *Proc. Natl. Acad. Sci. U.S.A. 104*, 13954−13959.

(41) Lai, C. K., Jeng, K. S., Machida, K., Cheng, Y. S., and Lai, M. M. (2008) Hepatitis C virus NS3/4A protein interacts with ATM, impairs DNA repair and enhances sensitivity to ionizing radiation. *Virology 370*, 295−309.

(42) Iwai, A., Takegami, T., Shiozaki, T., and Miyazaki, T. (2011) Hepatitis C virus NS3 protein can activate the Notch-signaling pathway through binding to a transcription factor, SRCAP. *PLoS One 6*, e20718.